M&C 2017 - International Conference on Mathematics & Computational Methods Applied to Nuclear Science & Engineering, Jeju, Korea, April 16-20, 2017, on USB (2017)

Bowing effects on power and burn-up distributions for simplified full PWR and BWR cores

D. Rochman,* P. Mala,* H. Ferroukhi,* A. Vasiliev,* M. Seidl,‡ D. Janin‡ and J. Li†

*Reactor Physics and Systems Behaviour Laboratory, Paul Scherrer Institut, Switzerland
‡Preussen Elektra GmbH, Hannover, Germany
†Graduate School of Engineering, The University of Tokyo, 113-8656 Tokyo, Japan
dimitri-alexandre.rochman@psi.ch*

Abstract - *In this paper, qualitative observations of the bowing effect are presented for two types of reactor core: one PWR and one BWR. The same bowing map is considered for both cores. The simulations are performed with the lattice code CASMO-5 and the bowing deformations are considered constant from the beginning to the end of the cycle. Different quantities such as the assembly power and some isotopic concentrations at the pin level are presented for a core burn-up of 15 MWd/kgU. This study shows that under the given assumptions, the bowing effect is stronger for the PWR pincell isotopic contents, whereas the assembly power is more affected in the case of the BWR core. Possible follow-up of this study are also presented.*

I. INTRODUCTION

Fuel assembly bowing has been observed at many instances in both Pressurized Water Reactor (PWR) and Boiling Water Reactor (BWR) [1, 2, 3]. Such a change of shape during the reactor service can have a negative influence on the motion of the control rods, can affect dry-out margins and therefore has an influence on the safety management. Additionally, geometry modifications induced by bowing contribute to the moderation variations and further impact on the neutronics characteristics of the fuel depletion, *e.g.* isotope inventory and power distribution. As a consequence, there is a potential impact for the fuel management during its handling after irradiation.

The evolution of the bowing amplitudes for single assemblies or as a common effect between groups of assemblies is not yet well understood and is therefore difficult to simulate. Many advanced dedicated studies from different institutes can be found in the literature, see for instance the 3D modeling at EDF with finite element analysis [4], analysis based on computational fluid dynamics [5, 6], or the experimental validation of the bowing effect for a BWR assembly [7].

Therefore different assumptions can be made based on experimental observations, as for instance presented in Ref. [8] for a bowing map measured from a EDF 1300 MW reactor. In the present work, we propose a simplified approach to model constant bowing amplitudes, based on a realistic bowing map for the PWR core as presented in Ref. [8]. As no bowing map is available for a BWR, the PWR is applied for both core types. Such reactor cores as presented in the following, although simplified as containing only fresh fuel, are made of a large number of fuel assemblies and are simulated up to a burn-up value of a few tens of MWd/kgU (only the results at 15 MWd/kgU are presented here). By using the same bowing map for both cores, it allows a straightforward comparison, even if the conclusions of this study should be treated with caution. The main goal of the study is to obtain a first qualitative assessment of the effects of assembly bowing on specific quantities.

In the following, the simulations are performed with the fuel assembly burn-up program CASMO-5 for both reactor types. Two calculation sets are performed: one nominal without any assembly displacement due to bowing, and one including individual assembly displacements following the measured PWR bowing map of Ref. [8]. We will first present the characteristics of the models and the assumed bowing map. Finally, results for the power map and the isotopic content for some nuclides at the pincell level will be presented.

II. NOMINAL MODELS

Two different core types are considered in this work: one PWR and one BWR. In this section are given the main characteristics of the cores without considering the bowing deformations. They are based on the examples provided in the CASMO-5 manual for the "MxN" model.

1. PWR full core

In this simplified PWR core, all the assemblies are considered the same and contains only UO_2 fresh fuel. Details are provided in Table I. The "M×N" model of CASMO-5 is used with full rectangular problem geometry. This multi-segment option allows to model an arbitrary array of assemblies. The control rods are not inserted and Method of Charac-

Assembly			
Geometry	17×17	Fuel pin R	0.4095
Fuel type	UO_2	Air gap R	0.4177
Rods	289	Clad R	0.475
Pitch (cm)	1.254	Clad	Zircaloy
Water channels	25	Clad ρ (g/cm^3)	6.56
Enrichment ^{235}U	4.11 %	Inner water R	0.57
Fuel ρ (g/cm^3)	10.07	Outer water R	0.615
Power dens. (W/gU)	25		
Core			
Assemblies	193	Geometry	17×17
Fuel T	900 K	Moderator T	600 K

TABLE I. Main characteristics of the PWR assemblies and core considered in this work. "R" means *radius*, given in cm.

teristics (MOC) is used for the 2-dimensional flux distribution for the entire problem.

2. BWR full core

As in the case of the PWR, the BWR core consists of similar assemblies, with UO_2 fresh fuel. Details are provided in Table II. As many fuel enrichments are used, the description is presented in Fig. 1. Among the 91 fuel rods, 9 contains Gadolinium with an enrichment of 2 %. Additionally, the average void in the coolant is constant for the whole burn-up calculations and equal to 41 %. Similarly to the PWR case, the "M×N" model is used and the control rods are not inserted. General layout of the full cores are represented in the following figures.

Bundle			
Geometry	10×10	Fuel pin R	0.442
Fuel type	UO_2	Air gap R	0.452
Rods	91	Clad R	0.502
Pitch (cm)	1.295	Clad	Zircaloy
Water Channel	9	Clad ρ (g/cm^3)	6.55
Wall dist. (cm)	13.4	Box Wall tick.	25 mm
Wide Water gap	2 cm	Narrow Water gap	1 cm
Fuel ρ (g/cm^3)	10.31	Power dens. (W/gU)	25
Core			
Assemblies	164	Geometry	16×16
Fuel T	900 K	Moderator T	559 K
Void coolant	41 %	Pressure	70 bar

TABLE II. Main characteristics of the BWR bundles and core considered in this work. "R" means *radius*, given in cm.

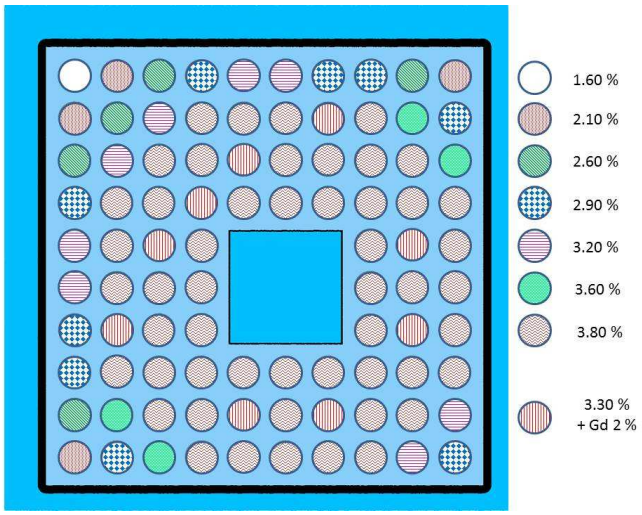

Fig. 1. Schematic view of the BWR bundle with different fuel enrichments as used in this work.

III. BOWING MODELS

The calculations are performed in a 2-Dimensional space. To simulate the bowing effect, each assembly can be displaced compared to its nominal location, for instance using the "*LDX*" and "*LDY*" cards in CASMO-5 for the PWR, or using the "*GAP*" card for the BWR. Both cards allows to obtain shifted locations of the assemblies compared to the original segment. Each simulation case is composed of the bowing model and the corresponding nominal model (without deformation) used as reference. All CASMO-5 calculations are performed with reflective boundary conditions. An example is presented in Fig. 2 for a simplified 3×3 assembly model for the BWR core. With a displacement of the central assembly parallel to one of its borders, one can achieve a bowing model with a single orientation. For a displacement occurring along two orthogonal borders simultaneously, a more realistic bowing model with an arbitrary orientation can be obtained. To visualize the displacement, only the regions adjacent to the central displaced assembly out of the 3×3 full assemblies model are shown in Fig. 2.

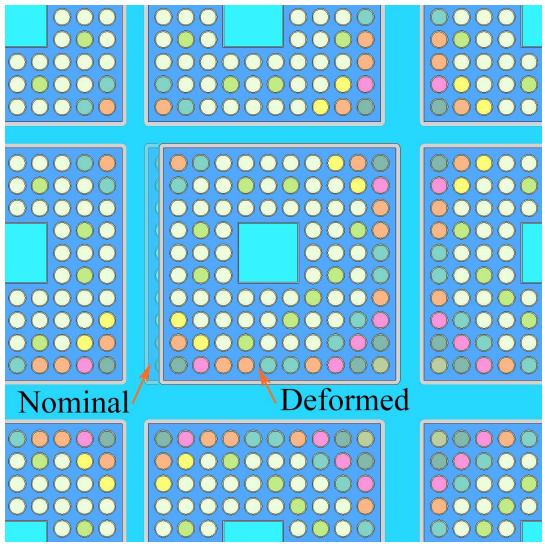

Fig. 2. A displaced central assembly and 8 surrounding assemblies with UO_2 fuels for BWR assemblies. Two arrows are indicating the positions of the original and displaced assemblies.

In terms of the restriction of the maximum displacement accessible with CASMO-5, orthogonal projections of displacements are scaled to be smaller than 1.5 mm for the full core models. The displacements are represented in the next figures by arrows on each assemblies. The length of the arrows is proportional to the displacement, see Figs. 3, 4 and 5. Same displacement maps are used for both reactor cores, but the size of the PWR core is larger than for the BWR core. Therefore the displacement map for the BWR is a subset of the one for the PWR: the maps are identical starting from the top left corner and is truncated for the BWR on the right and bottom sides.

The effect of the bowing map can be quantified by calculating the difference for the quantities of interest between the nominal case (no displacement) and the one with constant assembly displacements. Such results can be obtained for many quantities, such as the average isotopic contents in each as-

sembly, or the power distribution.
As the CASMO-5 simulations are performed up to a few tens of MWd/kgU, the evolution of the bowing effect can be followed for different burn-up rates, with the assumption of a constant assembly displacement. In a more real case, the bowing amplitude can vary as a function of the burn-up values, for instance linearly increasing, or following another function if experimental evidence exists.
In the next section, the results are presented. They depend on the assumed deformation magnitude which might not be representative of real core deformations.

IV. RESULTS

The CASMO-5 simulations are performed for both cores, each with two geometries (nominal and deformed) from 0 to 30 MWd/kgU. The quantities of interest presented here are the number densities for important isotopes: ^{148}Nd (for burn-up reconstruction), ^{235}U and ^{239}Pu (as main fissioning materials) and ^{244}Cm (of importance for the decay heat of spent fuel). Additionally, the effect of the bowing on the assembly power is also presented. Such calculations are rather calculational-demanding, compared to usual CASMO-5 calculations (CASMO-5 calculations are generally performed for "*cross section*" preparation at a single assembly level). As mentioned, the CASMO-5 "M×N" model is used for all the core assemblies at once, leading to relatively long calculation times (4-5 days on a single core) and large output files (up to 2 Gb).
In the following, results at 15 MWd/kgU are presented, being representative of the considered constant bowing effect for the whole irradiation time. All the figures present the results in the form of the differences (in %) between the deformed and the nominal geometry and a constant scale of -2.5 % to 2.5 % is chosen for all the figures. This allows an easy comparison between the different cases, even if some differences exceed this scale. This is not considered as a drawback as the main goal of this study is to qualitatively show the impact of the bowing effect.

1. Number densities

In the following, qualitative results are presented for the number densities of the four mentioned isotopes (see Figs. 3 and 4) at 15 MWd/kgU for the 2-Dimension PWR and BWR code models. These results are obtained based on the CASMO-5 models developed in Ref. [9]. The bowing amplitudes are obtained from Ref. [8].
For the isotopic content, the results are presented in terms of

$$\Delta = (C^D - C^N)/C^N, \quad (1)$$

where C^N is the isotope concentration from the nominal model, and C^D is the isotope concentration from the deformed model (with the bowing effect).
The magnitudes of Δ are dominated by the relative differences of the bowing amplitudes between adjacent assemblies. The direct effect of bowing assemblies is to modify the water gap, and therefore the moderation of neutrons. For water gap large enough, the amount of thermal neutrons and therefore the amount of fission (for ^{235}U and ^{239}Pu) and capture (for ^{238}U) will increase. Higher fission rates will lead to a deficiency of ^{235}U and ^{239}Pu whereas an increase of fission products (such as ^{148}Nd) compared to the nominal case. Higher capture rates on ^{238}U will lead to higher plutonium and curium contents. In the case of ^{239}Pu, a higher production is compensated by its disappearance by fission and capture. Therefore, ^{239}Pu follows the ^{235}U behavior. Following these observations, strong correlations should be observed for :

- gap increase $\Longleftrightarrow$ higher thermal neutron population
- gap increase $\Longleftrightarrow$ higher local power
- gap increase $\Longleftrightarrow \Delta(^{235}U) < 0$
- gap increase $\Longleftrightarrow \Delta(^{148}Nd) > 0$
- gap increase $\Longleftrightarrow \Delta(^{239}Pu) < 0$ (more capture)
- gap increase $\Longleftrightarrow \Delta(^{244}Cm) > 0$

(the text color follows the colors of Figs 3 and 4). The opposite effect, being the reduction of the gap, is also true. Such behavior is indeed observed for both the PWR and BWR. It can be noticed that the effect on ^{244}Cm is the highest, certainly due to its low concentration at 15 MWd/kgU. To quantify the maximum effects on the number densities, Table III presents the absolute value of the extremes as well as the averages for both reactor cores. As observed, the impact on ^{244}Cm is

	Extreme		Average	
	PWR	BWR	PWR	BWR
Pin ^{148}Nd	5.1	2.5	0.0	0.0
Pin ^{235}U	2.0	2.9	0.0	0.0
Pin ^{239}Pu	1.8	1.4	0.0	-0.1
Pin ^{244}Cm	21	8.0	-0.2	-0.3
Pin Power	5.5	1.8	0.0	0.0

TABLE III. Absolute values of Δ in % for the extreme variations of number densities, and average Δ, at 15 MWd/kgU.

the highest, while it is rather low on ^{239}Pu. Comparing both cores, the same bowing map leads to higher local isotopic variations in the case of the PWR, but the averages are all close to zero. Again, it should be emphasize that these values are obtained using a constant deformation as a function of the burn-up, which is certainly an over-estimation compared to a real case. These observations are likely to change in the case of a more realistic bowing representation, although the heavy actinides will be affected the most, as they strongly depend on the local power variations.
Regarding the assemblies at the periphery, auto-generated baffles are built by CASMO-5 at the sides adjacent to the outside water regions. Due to the baffle isolation, the bowing effects of these assemblies on the baffle side are more relevant to their own displacements.

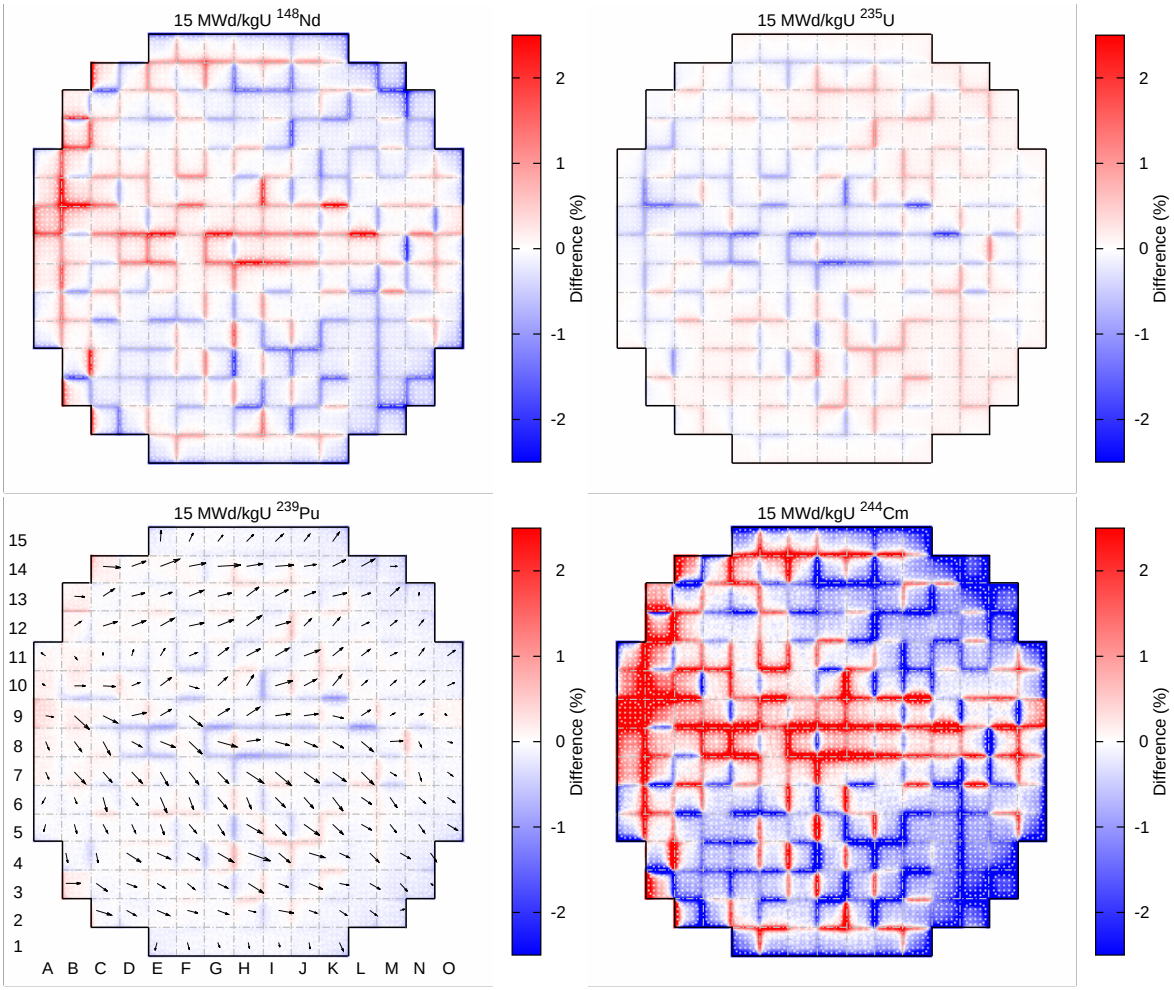

Fig. 3. Distributions of Δ for the 2D PWR full core models at 15 MWd/kgU. The differences between nominal and deformed configurations are presented for four isotopic content: ^{148}Nd, ^{235}U, ^{239}Pu and ^{244}Cm. Assembly displacements are indicated by arrows in the ^{239}Pu map. Note that the Z-scale is fixed to [-2.5;+2.5] %.

2. Average power

Fig. 5 presents the average power variations (following the same definition Δ) for the 2D PWR and BWR full core models at 15 MWd/kgU. Averages and extreme values for the assembly power are also presented in Table III. Same color identifications are used for the PWR and BWR, to emphasize the difference between the two cores. The first observation is that the effect on the assembly power is more pronounced in the case of the PWR, reaching a local extreme value of anout ± 5.5 %. In the case of the BWR core, the differences between the nominal and deformed configuration only lead to extremes of ± 1.8 %, almost 3 times lower than for the PWR. It is also interesting to notice that the location of the extreme values are roughly the same as in the case of the ^{148}Nd, emphasizing the effect of the local bowing at the assembly level. As for the number densities, such results may vary for different bowing assumptions as a function of the burn-up.

V. FUTURE WORK

This study represents a first step into the analysis and simulation of the bowing effect in the case of a 2D full core. Preliminary studies for 2D and 3D pincell and assemblies were previously performed in Ref. [9] at PSI, and many improvements to the current approach can be foreseen, as presented below.

- As the current studies focus on specific isotopes of importance of practical applications, such a study can easily be extended to a longer list.
- Different fuel types can be studied with part of core loaded with MOX fuel, if a realistic core loading is available.
- An observed bowing map is used in this study for the PWR core. In the case of the BWR, the same map is applied, even if it is known that the bowing amplitude is different for both reactor types. If available, a more

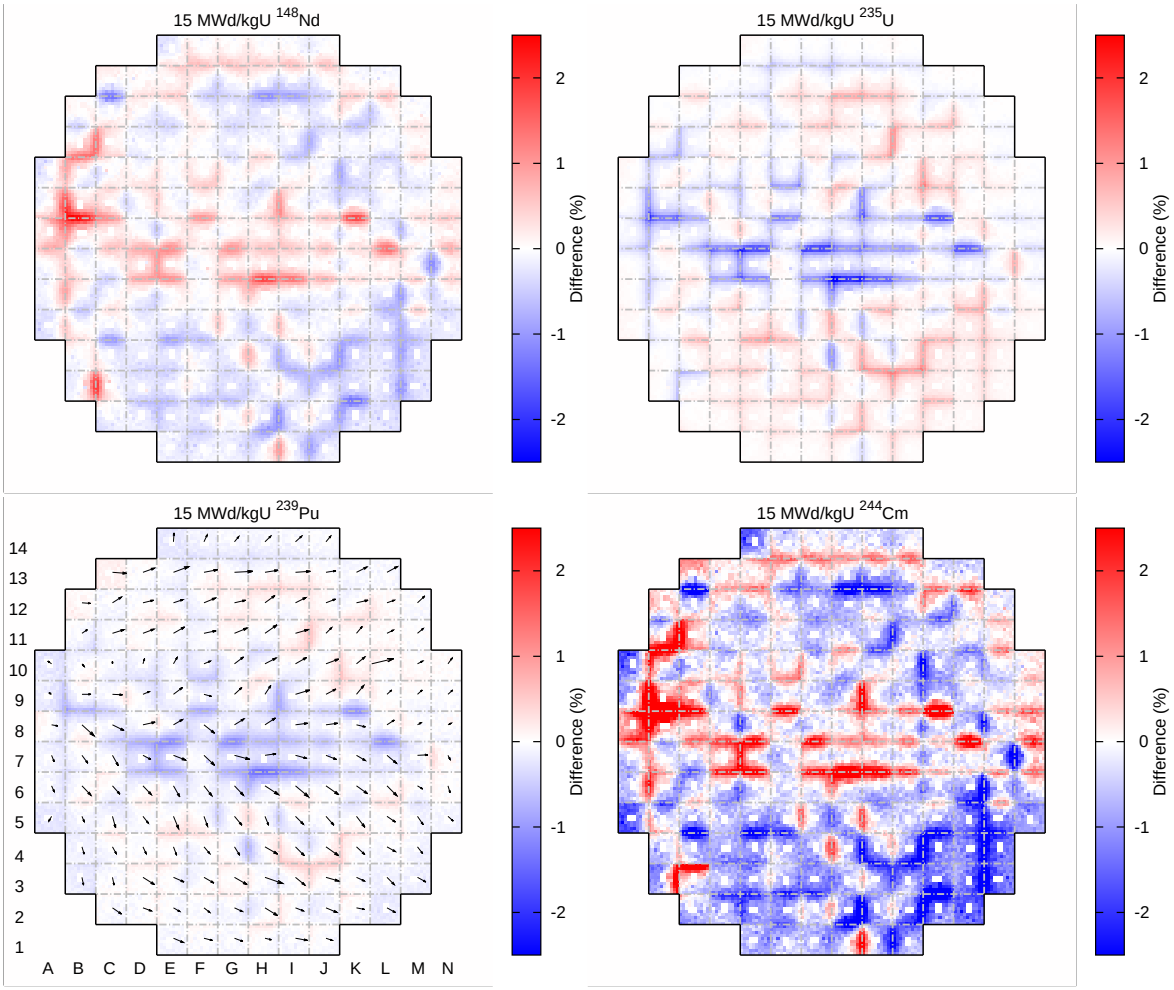

Fig. 4. Distributions of Δ for the 2D BWR full core models at 15 MWd/kgU. The differences between nominal and deformed configurations are presented for four isotopic content: ^{148}Nd, ^{235}U, ^{239}Pu and ^{244}Cm. Assembly displacements are indicated by arrows in the ^{239}Pu map. Note that the Z-scale is fixed to [-2.5;+2.5] %.

realistic bowing map should be used for the BWR.

- The bowing amplitude is considered constant as a function of the burn-up. This surely leads to an overestimation of the bowing impact on the local power and isotopic content. More realistic cases can nevertheless be simulated by changing the bowing amplitude with the irradiation time. If no measurements of the changing amplitude are available, assumptions such as a linearly increasing amplitude can be proposed and tested.
- In the case of the BWR core, different assembly geometries can be considered, such as the SVEA design. In this case, more elaborated deformation can also be tested.
- As shown in Ref. [10], bowing amplitudes are also changing from cycles to cycles, and depending on the assembly relocation. In this case, a single assembly can undergo very different bowing patterns. Simulations considering many cycles and the assembly location follow-up would be required.

It should be noticed that the study of the bowing effect is part of a general effort to assess the "*total*" uncertainty while performing full core simulations. Uncertainties on specific quantities arise from many sources (input parameters, irradiation histories, geometry assumptions, nuclear data, solver methods, *etc*). Examples of calculated uncertainties for full core calculations due to nuclear data can be found in Refs. [11, 12]. The bowing effect certainly affects many calculated values, as demonstrated here, and it is of importance to quantify and rank such impact compared to other sources. Ultimately, the global uncertainty assessment will help in core licensing and for safe and economical back-end fuel handling.

VI. CONCLUSION

This study focused on the bowing effect for the power distributions and isotopic content in the case of simplified full PWR and BWR cores. Preliminary simulations with CASMO-5 at 15 MWd/kgU have indicated that the bowing effect is of smaller impact for the pin power map for the

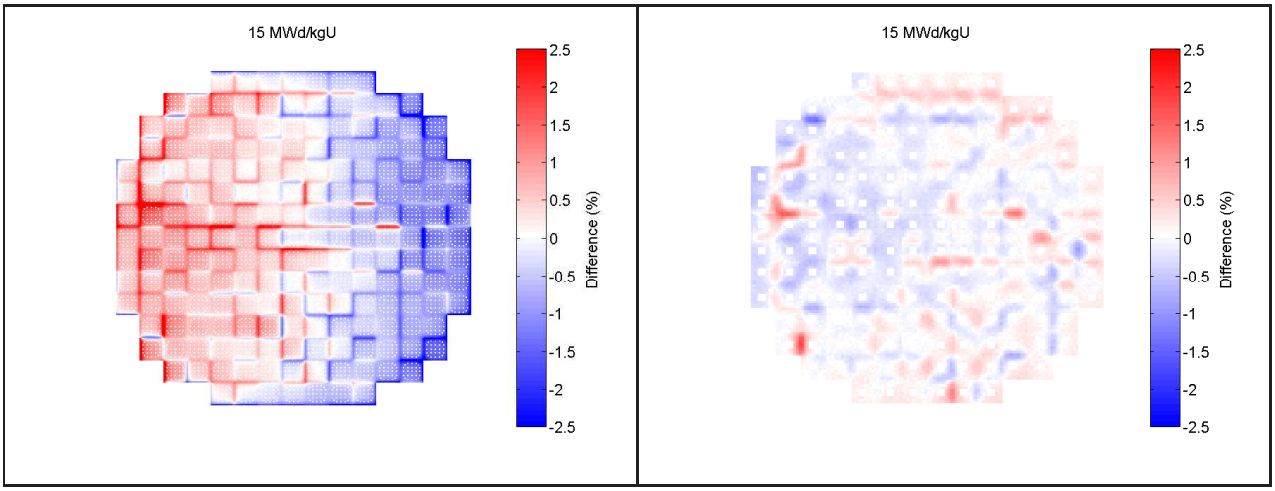

Fig. 5. Average power variations for the 2D full core models at 15 MWd/kgU. Left: PWR, right: BWR (using the same bowing amplitude map, represented by arrows in Figs. 3 and 4). Note that the Z-scale is fixed to [-2.5;+2.5] %.

BWR core (less than 2.0 %), but non negligible in the PWR case (maximum of 5.5 %). For the isotopic content, the effect is also stronger for the PWR core. These findings are subject to the following given assumptions: (1) fresh fuel for the full core and simplified hypothetical core design, and (2) constant bowing amplitude for the whole burn-up period. As presented, different simulation improvements are foreseen to have a better representation of the actual assembly bowing as a function of burn-up and for different cycles.

REFERENCES

1. S. T. MAHMOOD, Y. P. LIN, M. A. DUBECKY, K. EDSINGER, and E. MADER, "Channel Bow in Boiling Water Reactors - Hot Cell Examination Results and Correlation to Measured Bow," in "Proceedings of the 2007 LWR Fuel Performance," p. 124, san Francisco, United States, 2007.
2. S. Y. JEON, D. G. HA, J. K. PARK, K. B. EOM, and J. M. SUH, "The Effects of Fuel Design on the Fuel Assembly Bow Characteristics in PWR," in "Proceedings of the Korean Nuclear Society Spring Meeting," Jeju, Korea, May 17-18, 2012.
3. T. ANDERSSON, J. ALMBERGER, and L. BJORNKVIST, "A decade of assembly bow management at Ringhals," in "Proceedings of IAEA TM on Structural Behaviour of Fuel Assemblies for Water Cooled Reactors," .
4. B. LEVASSEUR, G. CHAIGNE, and R. FERNANDES, "3-D Modeling of Fuel Assemblies Growth and Bow for EDF PWRs," in "Proceedings of the Water Reactor Fuel Performance Meeting - WRFPM / Top Fuel 2009," Paris, France, 6-10 Sep. 2009.
5. A. PETRARCA, Y. ALESHIN, Y. XU, R. CORPAMASA, and J. GOMEZ-PALOMINO, "Effect of lateral hydraulic forces on fuel assembly bow," in "Proceedings of the Water Reactor Fuel Performance Meeting - Top Fuel 2015," Zurich, Switzerland, 13-17 Sep. 2015.
6. C. LASCAR, J. CHAMPIGNY, A. CHATELAIN, B. CHALOT, N. GOREAUD, E. MERY DE MONTIGNY, J. PACULL, and H. SALAUN, "Effect of lateral hydraulic forces on fuel assembly bow," in "Proceedings of the Water Reactor Fuel Performance Meeting - Top Fuel 2015," Zurich, Switzerland, 13-17 Sep. 2015.
7. P. GRIMM, F. JATUFF, M. MURPHY, R. SEILER, T. WILLIAMS, R. JACOT-GUILLARMOD, and R. CHAWLA, "Experimental Validation of Channel Bowing Effects on Pin Power Distributions in a Westinghouse SVEA-96+ Assembly," *Journal of Nuclear Science and Technology*, **43**, *3*, 223–230 (2006).
8. V. INOZEMTSEV, "Review of Fuel Failures in Water Cooled Reactors," Tech. Rep. IAEA Nuclear Energy Series No. NF-T-2.1, International Atomic Energy Agency (2010).
9. J. LI, *Simulations of Bowing Effects on isotopic inventories for simplified pin, assembly and full core models*, Master's thesis, Ecole Polytechnique de Lausanne, Lausanne, Switzerland (August 2016).
10. F. GARZORALLI, R. ADAMSON, P. RUDLING, and A. STRASSER, *BWR Fuel Channel Distortion*, Advanced Nuclear Technology International, Sweden (2011), www.antinternational.com/wp-content/uploads/ZIRAT16_STR_ChannelDistortion_sample1.pdf.
11. O. LERAY, A. V. H. FERROUKHI, M. HURSIN, and D. ROCHMAN, "Methodology for Core Analyses with Nuclear Data Uncertainty Quantification and Application to Swiss PWR Operated Cycles," *Annals of Nuclear Energy*, submitted in December 2016.
12. D. ROCHMAN, O. LERAY, M. HURSIN, H. FERROUKHI, A. VASILIEV, A. AURES, F. BOSTELMANN, W. ZWERMANN, O. CABELLOS, C. DIEZ, J. DYRDA, N. GARCIA-HERRANZ, E. CASTRO, S. VAN DER MARCK, H. SJOSTRAND, A. HERNANDEZ, M. FLEMING, J.-C. SUBLET, and L. FIORITO, "Nuclear Data Uncertainties for Typical LWR Fuel As-

semblies and a Simple Reactor Core," *Nuclear Data Sheets*, **139**, 1 – 76 (2017).